International Journal of Solids and Structures 118–119 (2017) 109–118

Contents lists available at ScienceDirect

International Journal of Solids and Structures

journal homepage: www.elsevier.com/locate/ijsolstr

A boundary-discontinuous-displacement based Fourier analysis of thick laminated beams via a robust 1D-CUF model

FG Canales[a], JL Mantari[a,b,*]

[a] Faculty of Mechanical Engineering, Universidad de Ingeniería y Tecnología (UTEC), Jr. Medrano Silva 165, Barranco, Lima, Perú
[b] University of New Mexico, Department of Mechanical Engineering, Albuquerque, New Mexico, U.S.A.

ARTICLE INFO

Article history:
Received 25 May 2016
Revised 1 April 2017
Available online 17 April 2017

Keywords:
Laminated beam
Analytical
Clamped
Boundary discontinuous
CUF

ABSTRACT

This paper presents an analytical solution for the static analysis of thick laminated rectangular beams with clamped boundary conditions at either or both of the beam's edges. A unified formulation known as Carrera's Unified Formulation (CUF) is used in order to consider shear deformation theories of arbitrary order. The governing equations are obtained by using the principle of virtual work. The main novelty is the use of the boundary-discontinuous Fourier approach for laminated beams in the framework of a unified formulation. Unlike Navier-type solutions, the present development can obtain analytical solutions for beams with clamped boundary conditions. A 3D finite element solution is used to validate the obtained results. The present theory can analyze clamped beams accurately so benchmark results are provided.

1. Introduction

Composite materials have many advantages compared to traditional metallic materials. Laminated composite beams are now widely used in aerospace and naval structures due to their lightness. However, composite beams have considerable transverse stress fields and thus require complex models to reproduce transverse stresses accurately. The classical or Euler-Bernoulli theory is inadequate to analyze these types of beams since this theory neglects transverse shear deformations. The Timoshenko beam theory is an improvement over the classical beam theory, but it requires a shear correction factor to correct the strain energy, as discussed by Hutchinson (1981), Hutchinson and Zillmer (1986) and Rychter (1987). In order to overcome the limitations of the Timoshenko beam theory, numerous higher order shear deformation theories (HSDTs) have been developed. HSDTs have nonuniform shear distribution in the beam's cross section, which can be captured by polynomial and non-polynomial shear strain shape functions. Khdeir and Reddy (1997) studied the bending of laminated beams using the Euler-Bernoulli theory and two HSDTs. Many other deformation theories have been developed for the analysis of composite laminated beams, and some are given in Sayyad and Ghugal (2011), Shimpi and Ghugal (2001), Aydogdu (2009) and Arya et al. (2002).

A unified formulation known as Carrera's Unified Formulation (CUF) has been developed by Carrera (2003). This formulation can analyze deformation theories of arbitrary order in a systematic manner, and it has been used to solve multifield problems (Carrera, 2005; Carrera et al., 2007, 2008). Beams are analyzed by using the one-dimensional CUF model, as presented in Carrera and Giunta (2010), Carrera et al. (2010) and Carrera and Petrolo (2012). Non-polynomial theories for beams have been developed by Carrera et al. (2013). This formulation can obtain quasi-3D solutions in many case problems. For example, accurate static (Catapano et al., 2011), free vibration (Giunta et al., 2013a; Filippi et al., 2015) and buckling analysis (Ibrahim et al., 2012) of laminated composite beams have been developed. The core of the formulation is given in Carrera et al. (2011) and Carrera et al. (2014). Special applications of 1D CUF models are given in Giunta et al. (2013b,c, 2016), Polit et al. (2015).

Analytical solutions are available for simply supported beams by using Navier-type solutions. Clamped boundary conditions can be considered in finite element solutions or by using the Ritz method, but these methods require analytical solutions to validate the results. Unlike simply supported boundary conditions, accurate analytical solutions for clamped boundary conditions are seldom developed, which represents a gap in the literature.

A method known as the boundary discontinuous Fourier method was developed by Chaudhuri (1989,2002) and it can be used to analyze beams with clamped boundary conditions. This method has been used for the analysis of cylindrical panels (Chaudhuri and Abu-Arja, 1991, Kabir and Chaudhuri, 1993), doubly-curved panels (Chaudhuri and Kabir, 1989; Kabir and

* Corresponding author.
E-mail addresses: jmantari@utec.edu, josemantari@gmail.com (J. Mantari).

http://dx.doi.org/10.1016/j.ijsolstr.2017.04.017
0020-7683/

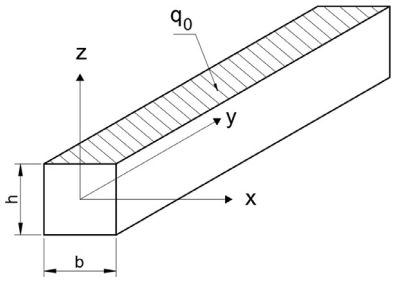

Fig. 1. Coordinate frame of the beam model.

Chaudhuri, 1991b; Chaudhuri and Kabir, 1992; Chaudhuri and Kabir, 1993c,d,e 1994; Kabir and Chaudhuri, 1994) and plates (Chaudhuri and Kabir, 1993a,b; Kabir and Chaudhuri, 1991a; Chaudhuri, 1994; Kabir, 1994; Chaudhuri et al., 2005). The discontinuities introduced reduce the speed of convergence of the Fourier series, and in order to balance this issue mixed Fourier solutions have been developed in (Chaudhuri and Kabir, 2005; Kabir et al., 2003) which have superior rate of convergence. The boundary discontinuous Fourier method has been applied for the analysis of plates and shells using HSDTs, as presented in Oktem and Chaudhuri (2007a,b,c, 2008, 2009).

In this paper, an analytical solution for the static analysis of composite thick beams with clamped boundary conditions at either or both of the beam's edges is obtained. The displacement field is expressed within the framework of CUF in order to consider theories of arbitrary order in a systematic manner. The governing equations are obtained by using the principle of virtual work. The validity of the results is assessed by analyzing the convergence of the results and by comparing the present results with a 3D finite element solution. Good agreement of the results between the present model and 3D finite element solution is obtained. Consequently, the present results can be used as benchmark for comparison with approximate solution methods.

2. Analytical modeling

A beam of length L, width b and a total thickness h is considered in the present analysis. The rectangular cartesian coordinate system used in the present work is shown in Fig. 1. The beam occupies the following region:

$$-b/2 \le x \le b/2; \qquad 0 \le y \le L; \qquad -h/2 \le z \le h/2$$

2.1. Elastic stress-strain relations

A general displacement vector is introduced:

$$\mathbf{u}(x, y, z) = \left\{u_x \quad u_y \quad u_z\right\}^T \tag{1}$$

The cross-sectional plane of the beam is denoted by Ω. The stress and strain vectors are expressed as follows:

$$\begin{aligned}\sigma &= \left\{\sigma_{zz} \quad \sigma_{xx} \quad \sigma_{xz} \quad \sigma_{zy} \quad \sigma_{xy} \quad \sigma_{yy}\right\}^T \\ \varepsilon &= \left\{\varepsilon_{zz} \quad \varepsilon_{xx} \quad \varepsilon_{xz} \quad \varepsilon_{zy} \quad \varepsilon_{xy} \quad \varepsilon_{yy}\right\}^T\end{aligned} \tag{2}$$

The constitutive equation can be written as follows:

$$\sigma = \tilde{\mathbf{C}}\varepsilon \tag{3}$$

where $\tilde{\mathbf{C}}$ is a matrix of stiffness coefficients. For an orthotropic material, it is given by:

$$\tilde{\mathbf{C}} = \begin{bmatrix} \tilde{C}_{11} & \tilde{C}_{12} & 0 & 0 & 0 & \tilde{C}_{13} \\ \tilde{C}_{12} & \tilde{C}_{22} & 0 & 0 & 0 & \tilde{C}_{23} \\ 0 & 0 & \tilde{C}_{44} & 0 & 0 & 0 \\ 0 & 0 & 0 & \tilde{C}_{55} & 0 & 0 \\ 0 & 0 & 0 & 0 & \tilde{C}_{66} & 0 \\ \tilde{C}_{13} & \tilde{C}_{23} & 0 & 0 & 0 & \tilde{C}_{33} \end{bmatrix} \tag{4}$$

The orientation of the laminas is defined using the Y axis as a reference. Only laminated materials with cross-ply layups, i.e. with laminas oriented at 0 or 90° from the Y axis, can be analyzed using the present boundary-discontinuous method. The limitation is similar as for Navier-type solutions. For ease of development, the stress and strain vectors in Eq. (2) are partitioned:

$$\begin{aligned}\sigma_p &= \left\{\sigma_{zz} \quad \sigma_{xx} \quad \sigma_{xz}\right\}^T, \varepsilon_p = \left\{\varepsilon_{zz} \quad \varepsilon_{xx} \quad \varepsilon_{xz}\right\}^T \\ \sigma_n &= \left\{\sigma_{zy} \quad \sigma_{xy} \quad \sigma_{yy}\right\}^T, \varepsilon_n = \left\{\varepsilon_{zy} \quad \varepsilon_{xy} \quad \varepsilon_{yy}\right\}^T\end{aligned} \tag{5}$$

Considering small amplitude displacements, the strain are given by:

$$\varepsilon_p = \begin{Bmatrix} u_{z,z} \\ u_{x,x} \\ u_{x,z} + u_{z,x} \end{Bmatrix}, \varepsilon_n = \begin{Bmatrix} u_{y,z} + u_{z,y} \\ u_{y,x} + u_{x,y} \\ u_{y,y} \end{Bmatrix} \tag{6}$$

where the comma denotes a partial derivative. Using vector notation, Eq. (6) can be expressed as:

$$\begin{aligned}\varepsilon_p &= \mathbf{D}_p\mathbf{u} \\ \varepsilon_n &= \mathbf{D}_n\mathbf{u} = (\mathbf{D}_{n\Omega} + \mathbf{D}_{ny})\mathbf{u}\end{aligned} \tag{7}$$

The subscript "*p*" stands for terms lying on planes orthogonal to the cross-section, while the subscript "*n*" stands for terms lying on the cross section. The linear differential operators $\mathbf{D}_p$, $\mathbf{D}_{n\Omega}$ and $\mathbf{D}_{ny}$ are given by:

$$\begin{aligned}\mathbf{D}_p &= \begin{bmatrix} 0 & 0 & \frac{\partial}{\partial z} \\ \frac{\partial}{\partial x} & 0 & 0 \\ \frac{\partial}{\partial z} & 0 & \frac{\partial}{\partial x} \end{bmatrix}, \mathbf{D}_{n\Omega} = \begin{bmatrix} 0 & \frac{\partial}{\partial z} & 0 \\ 0 & \frac{\partial}{\partial x} & 0 \\ 0 & 0 & 0 \end{bmatrix} \\ \mathbf{D}_{ny} &= \begin{bmatrix} 0 & 0 & \frac{\partial}{\partial y} \\ \frac{\partial}{\partial y} & 0 & 0 \\ 0 & \frac{\partial}{\partial y} & 0 \end{bmatrix}\end{aligned} \tag{8}$$

The constitutive equation, given by Eq. (3), can be split by using the partition of the stress and strain vectors given in Eq. (5):

$$\begin{aligned}\sigma_p &= \tilde{\mathbf{C}}_{pp}\varepsilon_p + \tilde{\mathbf{C}}_{pn}\varepsilon_n \\ \sigma_n &= \tilde{\mathbf{C}}_{np}\varepsilon_p + \tilde{\mathbf{C}}_{nn}\varepsilon_n\end{aligned} \tag{9}$$

The matrices $\tilde{\mathbf{C}}_{pp}$, $\tilde{\mathbf{C}}_{pn}$, $\tilde{\mathbf{C}}_{np}$ and $\tilde{\mathbf{C}}_{nn}$ are obtained as partitions of Eq. (4), and are given by:

Table 1
MacLaurin's polynomials.

N	M	F_τ
0	1	$F_1=1$
1	3	$F_2=x,\ F_3=z$
2	6	$F_4=x^2, F_5=xz,\ F_6=z^2$
3	10	$F_7=x^3, F_8=x^2z, F_9=xz^2, F_{10}=z^3$
...	...	...
N	$\frac{(N+1)(N+2)}{2}$	$F_{(N^2+N+2)/2}=x^N,\ F_{(N^2+N+4)/2}=x^{N-1}z ... F_{N(N+3)/2}=xz^{N-1},$ $F_{(N+1)(N+2)/2}=z^N$

$$\tilde{\mathbf{C}}_{pp}=\begin{bmatrix}\tilde{C}_{11} & \tilde{C}_{12} & 0\\ \tilde{C}_{12} & \tilde{C}_{22} & 0\\ 0 & 0 & \tilde{C}_{44}\end{bmatrix},\tilde{\mathbf{C}}_{nn}=\begin{bmatrix}\tilde{C}_{55} & 0 & 0\\ 0 & \tilde{C}_{66} & 0\\ 0 & 0 & \tilde{C}_{33}\end{bmatrix}$$
$$\tilde{\mathbf{C}}_{pn}=\tilde{\mathbf{C}}_{np}^{T}=\begin{bmatrix}0 & 0 & \tilde{C}_{13}\\ 0 & 0 & \tilde{C}_{23}\\ 0 & 0 & 0\end{bmatrix} \tag{10}$$

The coefficients $\tilde{C}_{ij}$ depend on the material properties. They can be found in standard texts of laminated materials, as presented in Reddy (2004).

2.2. Displacement field

The displacement field is expressed within the framework of the CUF:

$$\mathbf{u}(x,y,z)=F_\tau(x,z)\mathbf{u}_\tau(y)\qquad \tau=1,2,...,M \tag{11}$$

where F_τ are functions of the coordinates x and z on the cross-section, M stands for the number of terms used in the expansion, $\mathbf{u}_\tau$ is the vector of the generalized displacements, and the repeated subscript "τ" indicates summation. A Taylor-type expansion is used to determine the functions F_τ, consisting on Maclaurin series that uses the 2D polynomials x^iz^j as base. Table 1 shows M and F_τ as functions of the order expansion N. For example, the displacement field of the second-order (N=2) Taylor-type expansion model can be expressed as:

$$\begin{aligned}u_x&=u_{x_1}+xu_{x_2}+zu_{x_3}+x^2u_{x_4}+xzu_{x_5}+z^2u_{x_6}\\ u_y&=u_{y_1}+xu_{y_2}+zu_{y_3}+x^2u_{y_4}+xzu_{y_5}+z^2u_{y_6}\\ u_z&=u_{z_1}+xu_{z_2}+zu_{z_3}+x^2u_{z_4}+xzu_{z_5}+z^2u_{z_6}\end{aligned} \tag{12}$$

2.3. Principle of virtual work

The static version of the principle of virtual work is applied:

$$\delta L_{int}=\int_V\left(\delta\varepsilon_p^T\sigma_p+\delta\varepsilon_n^T\sigma_n\right)dV=\delta L_{ext} \tag{13}$$

where δ stands for the virtual variation operator, L_{int} stands for the strain energy and L_{ext} is the external virtual work. Substituting Eqs. (7) and (9) in Eq. (13) the following expression is obtained:

$$\begin{aligned}\delta L_{int}=&\int_y\int_\Omega\left\{[\mathbf{D}_p\delta\mathbf{u}]^T\left[\tilde{\mathbf{C}}_{pp}\mathbf{D}_p+\tilde{\mathbf{C}}_{pn}(\mathbf{D}_{n\Omega}+\mathbf{D}_{ny})\right]\mathbf{u}\right.\\ &\left.+[(\mathbf{D}_{n\Omega}+\mathbf{D}_{ny})\delta\mathbf{u}]^T\left[\tilde{\mathbf{C}}_{np}\mathbf{D}_p+\tilde{\mathbf{C}}_{nn}(\mathbf{D}_{n\Omega}+\mathbf{D}_{ny})\right]\mathbf{u}\right\}d\Omega dy\\ =&\ \delta L_{ext}\end{aligned} \tag{14}$$

Substituting Eqs. (11) and (10) in Eq. (14) and integrating by parts results in the following:

$$\delta L_{int}=\int_y\delta\mathbf{u}_s^T\mathbf{K}^{\tau s}\mathbf{u}_\tau dy+\left[\delta\mathbf{u}_s^T\Pi^{\tau s}\mathbf{u}_\tau\right]_{y=0}^{y=L}=\delta L_{ext} \tag{15}$$

where $\mathbf{K}^{\tau s}$ is the stiffness matrix and $\Pi^{\tau s}$ is the matrix of the natural boundary conditions. The components of $\mathbf{K}^{\tau s}$ are provided as follows:

$$\begin{aligned}K_{(11)}^{\tau s}&=E_{\tau,_xs,_x}^{22}+E_{\tau,_zs,_z}^{44}-E_{\tau s}^{66}\frac{\partial^2}{\partial y^2}\\ K_{(12)}^{\tau s}&=E_{\tau,_xs}^{23}\frac{\partial}{\partial y}-E_{\tau s,_x}^{66}\frac{\partial}{\partial y}\\ K_{(13)}^{\tau s}&=E_{\tau,_xs,_z}^{12}+E_{\tau,_zs,_x}^{44}\\ K_{(21)}^{\tau s}&=E_{\tau,_xs}^{66}\frac{\partial}{\partial y}-E_{\tau s,_x}^{23}\frac{\partial}{\partial y}\\ K_{(22)}^{\tau s}&=E_{\tau,_zs,_z}^{55}+E_{\tau,_xs,_x}^{66}-E_{\tau s}^{33}\frac{\partial^2}{\partial y^2}\\ K_{(23)}^{\tau s}&=E_{\tau,_zs}^{55}\frac{\partial}{\partial y}-E_{\tau s,_z}^{13}\frac{\partial}{\partial y}\\ K_{(31)}^{\tau s}&=E_{\tau,_zs,_x}^{12}+E_{\tau,_xs,_z}^{44}\\ K_{(32)}^{\tau s}&=E_{\tau,_zs}^{13}\frac{\partial}{\partial y}-E_{\tau s,_z}^{55}\frac{\partial}{\partial y}\\ K_{(33)}^{\tau s}&=E_{\tau,_zs,_z}^{11}+E_{\tau,_xs,_x}^{44}-E_{\tau s}^{55}\frac{\partial^2}{\partial y^2}\end{aligned} \tag{16}$$

where a cross-sectional moment parameter has been used, and a generic term is defined below:

$$E_{\tau,_\gamma s,_\theta}^{\alpha\beta}=\int_\Omega\tilde{C}_{\alpha\beta}F_{\tau,\gamma}F_{s,\theta}d\Omega \tag{17}$$

The components of $\Pi^{\tau s}$ are provided as follows:

$$\begin{aligned}&\Pi_{(11)}^{\tau s}=E_{\tau s}^{66}\frac{\partial}{\partial y}\quad \Pi_{(12)}^{\tau s}=E_{\tau s,_x}^{66}\quad \Pi_{(13)}^{\tau s}=0\\ &\Pi_{(21)}^{\tau s}=E_{\tau s,_x}^{23}\quad \Pi_{(22)}^{\tau s}=E_{\tau s}^{33}\frac{\partial}{\partial y}\quad \Pi_{(23)}^{\tau s}=E_{\tau s,_z}^{13}\\ &\Pi_{(31)}^{\tau s}=0\quad \Pi_{(32)}^{\tau s}=E_{\tau s,_z}^{55}\quad \Pi_{(33)}^{\tau s}=E_{\tau s}^{55}\frac{\partial}{\partial y}\end{aligned} \tag{18}$$

Letting $\mathbf{P}_\tau=\{\mathbf{P}_{x\tau}\mathbf{P}_{y\tau}\mathbf{P}_{z\tau}\}^T$ define a vector of generalized forces, the natural boundary conditions can be obtained by substituting Eq. (18) in Eq. (15):

$$\delta u_{xs}:\qquad P_{x\tau}=E_{\tau s}^{66}u_{x\tau,y}+E_{\tau s,_x}^{66}u_{y\tau} \tag{19a}$$

$$\delta u_{ys}:\qquad P_{y\tau}=E_{\tau s,_x}^{23}u_{x\tau}+E_{\tau s}^{33}u_{y\tau,y}+E_{\tau s,_z}^{13}u_{z\tau} \tag{19b}$$

$$\delta u_{zs}:\qquad P_{z\tau}=E_{\tau s,_z}^{55}u_{y\tau}+E_{\tau s}^{55}u_{z\tau,y} \tag{19c}$$

2.4. Boundary discontinuous solution

Geometric boundary conditions for simply supported beams, in terms of the displacement variables given in Eq. (11), are expressed as:

$$\begin{aligned}u_{x\tau}(0)=u_{y\tau,y}(0)=u_{z\tau}(0)=0\\ u_{x\tau}(L)=u_{y\tau,y}(L)=u_{z\tau}(L)=0\end{aligned} \tag{20}$$

Geometric boundary conditions for clamped – clamped beams, in terms of the displacement variables given in Eq. (11) are additional constraints to those given in Eq. (20):

$$u_{y\tau}(0)=0 \tag{21a}$$

$$u_{y\tau}(L)=0 \tag{21b}$$

The displacement variables are assumed as follows:

$$u_{x\tau} = \sum_{m=1}^{p} U_{x\tau m} \sin(\alpha_m y) \qquad 0 \le y \le L \tag{22a}$$

$$u_{y\tau} = \sum_{m=0}^{p} U_{y\tau m} \cos(\alpha_m y) \qquad 0 < y < L \tag{22b}$$

$$u_{z\tau} = \sum_{m=1}^{p} U_{z\tau m} \sin(\alpha_m y) \qquad 0 \le y \le L \tag{22c}$$

where m is the wave number of the trigonometric term and p the number of trigonometric terms of the series. The coefficient α_m is given by:

$$\alpha_m = \frac{m\pi}{L} \tag{23}$$

The total number of unknown Fourier coefficients introduced in Eqs. (22) is M(3p+1). The assumed solution satisfies the simply supported boundary condition given in Eq. (20). However, the clamped support boundary condition, given in Eq. (21), is not satisfied. In order to obtain analytical solution for clamped beams, the boundary discontinuous method is used. The details of the procedure are given in Refs. Chaudhuri (1989, 2002).

The boundary discontinuous method introduces boundary Fourier coefficients arising from discontinuities of the solution at the edges y=0, L. The displacement variable $u_{y\tau}$, as defined by Eq. (22b), does not satisfy the boundary condition for clamped supports given in Eq. (21). Therefore, it is forced to vanish at these edges. The partial derivative $u_{y\tau,y}$ is seen to vanish at the edges, thus violating the complementary boundary constraint or boundary discontinuities at these edges; see Chaudhuri (1989, 2002). For further differentiation, $u_{y\tau,yy}$ is expanded in a Fourier series in order to satisfy the complementary boundary constraint. It is important to note that the derivative of the Fourier series of a given function is not necessarily the same as the Fourier series of the derivative of the function when this function has discontinuities.

The Fourier series of the partial derivative $u_{y\tau,y}$ is given by:

$$u_{y\tau,y} = \sum_{m=1}^{p} U_{y\tau m,y} \sin(\alpha_m y) \qquad 0 < y < L \tag{24a}$$

$$U_{y\tau m,y} = \frac{2}{L}\int_0^L u_{y\tau,y} \sin(\alpha_m y)dy \tag{24b}$$

where $U_{y\tau m,y}$ is the Fourier term associated with the Fourier series of the function $u_{y\tau,y}$. Integrating Eq. (24b) by parts and using the vanishing boundary conditions given in Eq. (21):

$$\begin{aligned} U_{y\tau m,y} &= \frac{2}{L} u_{y\tau} \sin(\alpha_m y)|_{y=0}^{y=L} - \frac{2}{L}\int_0^L u_{y\tau}\alpha_m \cos(\alpha_m y)dy \\ U_{y\tau m,y} &= -(\alpha_m)\frac{2}{L}\int_0^L u_{y\tau} \cos(\alpha_m y)dy \end{aligned} \tag{25}$$

The Fourier term $U_{y\tau m}$ of the Fourier series of the function $u_{y\tau}$ is recognized:

$$U_{y\tau m,y} = -\alpha_m U_{y\tau m} \tag{26}$$

Thus, the first partial derivative can be obtained through term-by-term differentiation. The Fourier series of the second partial derivative $u_{y\tau,yy}$ is given by:

$$u_{y\tau,yy} = \frac{1}{2}a_\tau + \sum_{m=1}^{p} U_{y\tau m,yy} \cos(\alpha_m y) \qquad 0 < y < L \tag{27a}$$

$$U_{y\tau m,yy} = \frac{2}{L}\int_0^L u_{y\tau,yy} \cos(\alpha_m y)dy \tag{27b}$$

where $U_{y\tau m,yy}$ is the Fourier term of the function $u_{y\tau,yy}$ and a_τ is a Fourier coefficient. Integrating Eq. (27b) by parts, the following expression is obtained:

$$U_{y\tau m,yy} = \frac{2}{L} u_{y\tau,y} \cos(\alpha_m y)|_{y=0}^{y=L} + \frac{2}{L}\int_0^L u_{y\tau,y}\alpha_m \sin(\alpha_m y)dy \tag{28}$$

Note that the function $u_{y\tau,y}$ does not necessarily vanish at the edges (contrary to what may be suggested by Eq. (22b)) since discontinuities are introduced at y=0, *L*. Substituting Eqs. (24b) and (26) in Eq. (28) the Fourier term is obtained as:

$$U_{y\tau m,yy} = \frac{2}{L}\left[(-1)^m u_{y\tau,y}(L) - u_{y\tau,y}(0)\right] - \alpha_m^2 U_{y\tau m} \tag{29}$$

Substituting Eq. (29) in Eq. (27a) the following expression is obtained:

$$u_{y\tau,yy} = \frac{1}{2}a_\tau + \sum_{m=1}^{p}\left(-\alpha_m^2 U_{y\tau m} + \gamma_m a_\tau + \psi_m b_\tau\right)\cos(\alpha_m y) \tag{30}$$

where the Fourier coefficients a_τ and b_τ introduce 2M new unknowns. These coefficients are given by:

$$a_\tau = \frac{2}{L}[u_{y\tau,y}(L) - u_{y\tau,y}(0)] \tag{31a}$$

$$b_\tau = -\frac{2}{L}[u_{y\tau,y}(L) + u_{y\tau,y}(0)] \tag{31b}$$

and γ_m,ψ_m are defined as:

$$(\gamma_m, \psi_m) = \begin{cases} (1,0), & m = \text{even} \\ (0,1), & m = \text{odd} \end{cases} \tag{32}$$

2.5. Virtual work of the load

The external work of the uniform load q_0 applied in the surface z=h/2 (see Fig. 1) is given by:

$$\delta L_{ext} = \int_0^L \int_{-b/2}^{b/2} q_0 \delta u_z|_{z=h/2} dxdy \tag{33}$$

Substituting Eq. (11) in Eq. (33):

$$\delta L_{ext} = \delta u_{sz}\int_0^L \left(\int_{-b/2}^{b/2} q_0 F_{sz}|_{z=h/2} dx\right)dy \tag{34}$$

The load is expressed using a Fourier series:

$$q_0 = \sum_{m=1}^{p} Q_m \sin(\alpha_m y), \qquad Q_m = \frac{2}{L}\int_0^L q_0 \sin(\alpha_m y)dy \tag{35}$$

where Q_m is a Fourier coefficient associated with the Fourier series of the load. Other types of loads can be analyzed in a similar manner, see Ref. Carrera and Giunta (2010).

2.6. Governing equations

Substituting Eqs. (22) and their appropriate partial derivatives in Eq. (15), in conjunction with Eqs. (16), (30), (34) and (35), the following expressions are obtained:

$$\begin{aligned} &\sum_{m=1}^{p} \sin(\alpha_m y)\Big\{\left(E^{22}_{\tau,xs_x} + E^{44}_{\tau,zs_z} + E^{66}_{\tau s}\alpha_m^2\right)U_{x\tau m} \\ &+ \left(-E^{23}_{\tau,xs}\alpha_m + E^{66}_{\tau s_x}\alpha_m\right)U_{y\tau m}\left(E^{12}_{\tau,xs_z} + E^{44}_{\tau,zs_x}\right)U_{z\tau m}\Big\} = 0 \end{aligned} \tag{36a}$$

$$\sum_{m=1}^{p} \cos(\alpha_m y)\Big\{\big(E^{66}_{\tau,xs}\alpha_m - E^{23}_{\tau s,x}\alpha_m\big)U_{x\tau m} + \big(E^{55}_{\tau,zs,z} + E^{66}_{\tau,xs,x} + E^{33}_{\tau s}\alpha_m^2\big) \times U_{y\tau m}\big(E^{55}_{\tau,zs}\alpha_m - E^{13}_{\tau s,z}\alpha_m\big)U_{z\tau m} - E^{33}_{\tau s}(\gamma_m a_\tau + \psi_m b_\tau)\Big\} = 0 \tag{36b}$$

$$\sum_{m=1}^{p} \sin(\alpha_m y)\left\{\big(E^{12}_{\tau,zs,x} + E^{44}_{\tau,xs,z}\big)U_{x\tau m} + \big(-E^{13}_{\tau,zs}\alpha_m + E^{55}_{\tau s,z}\alpha_m\big)U_{y\tau m} \times \big(E^{11}_{\tau,zs,z} + E^{44}_{\tau,xs,x} + E^{55}_{\tau s}\alpha_m^2\big)U_{z\tau m} - Q_m\left(\int_{-b/2}^{b/2} F_{\tau z}|_{z=h/2}dx\right)\right\} = 0 \tag{36c}$$

$$-E^{33}_{\tau s}\frac{a_\tau}{2} + \big(E^{55}_{\tau,zs,z} + E^{66}_{\tau,xs,x}\big)U_{y\tau 0} = 0 \tag{37}$$

Equating the coefficients of the trigonometric functions of Eqs. (36) and (37) to zero yields to M(3p+1) linear algebraic equations. Additional equations are supplied by the geometric boundary conditions relating to vanishing of the displacement variables $u_{y\tau}$ at the edges y=0, L (due to the clamped boundary conditions). Using Eq. (22b):

$$u_{y\tau}(0) = 0 \quad \rightarrow \quad \sum_{m=0}^{p} U_{y\tau m} = 0 \tag{38a}$$

$$u_{y\tau}(L) = 0 \quad \rightarrow \quad \sum_{m=0}^{p} (-1)^m U_{y\tau m} = 0 \tag{38b}$$

These equations can be expressed in a more convenient form, as in Oktem and Chaudhuri (2007c):

$$U_{y\tau 0} + \sum_{m=2,4,\ldots}^{p} U_{y\tau m} = 0 \tag{39a}$$

$$\sum_{m=1,3,\ldots}^{p} U_{y\tau m} = 0 \tag{39b}$$

This step generates 2M additional equations, resulting in a total of M(3p+3) linear algebraic equations in as many unknowns.

2.7. Extension to other boundary conditions

In addition to the clamped – clamped boundary condition, a beam with clamped – simply supported boundary conditions can also be analyzed by the present method. A clamped edge is considered at y=0 and a simply supported edge at y=L. Since the boundary condition given in Eq. (21b) has been relaxed, the function $u_{y\tau}$ is no longer forced to vanish at y=L and Eq. (38b) is no longer needed. This step reduces the available equations in M compared to the clamped – clamped case. In addition, $u_{y\tau,y}$ no longer has a discontinuity at y=L and it is equal to zero at this point. By substituting $u_{y\tau,y}(L)=0$ in Eqs. (31), the following relation is obtained:

$$a_\tau = b_\tau \tag{40}$$

This step eliminates M unknowns, and thus the system remains determinate. For a simply supported beam, Eqs. (38a) and (38b) are no longer required, reducing the available equations in 2M compared to the clamped – clamped case. In addition, $u_{y\tau,y}$ no longer has discontinuities at y=0, L and it is equal to zero at these points. By substituting $u_{y\tau,y}(0)=u_{y\tau,y}(L)=0$ in Eqs. (31), the following relation is obtained:

$$a_\tau = b_\tau = 0 \tag{41}$$

This step eliminates 2M unknowns, and thus the system remains determinate. The remaining governing equations, given by Eqs. (36a–c), are the same as for a Navier-type solution. Consequently, the present method can be considered a generalization of the Navier solution.

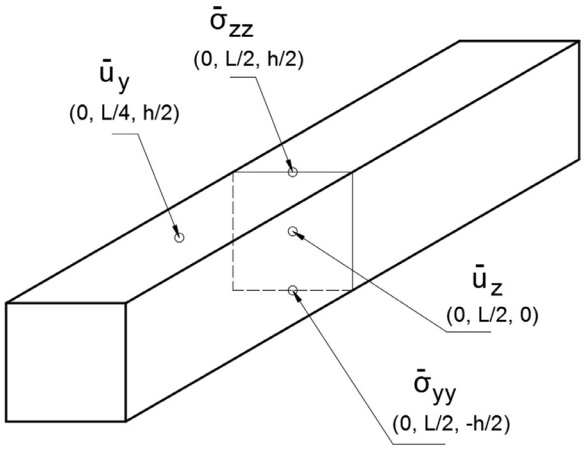

Fig. 2. Points of evaluation of the transverse displacement $\bar{u}_z$, axial stress $\bar{\sigma}_{yy}$, axial displacement $\bar{u}_y$ and transverse normal stress $\bar{\sigma}_{zz}$.

3. Numerical results and discussion

3.1. Material properties and normalization

An orthotropic (0/90°) laminated square beam subjected to a uniform load is considered in the following numerical examples. The following material properties are used:

$$\frac{E_y}{E_x} = 25,\ \frac{E_z}{E_x} = 1,\ \frac{G_{xy}}{E_x} = \frac{G_{yz}}{E_x} = 0.5$$
$$\frac{G_{xz}}{E_x} = 0.2,\ \nu_{xy} = 0.01 \qquad \nu_{xz} = \nu_{yz} = 0.25 \tag{42}$$

where E_i are the Young's modulus of elasticity, ν_{ij} are the Poisson's ratios and G_{ij} are the shear modulus of elasticity. The subscripts indicate the axes of the elastic constants. The displacements, stresses and geometric parameters are expressed in the following non-dimensional form:

$$\bar{u}_z = 10^2 \times \frac{E_x h^3}{q_0 L^4} u_z,\ \bar{u}_y = 10^3 \times \frac{E_x h^3}{q_0 L^4} u_y$$
$$\bar{\sigma}_{yy} = 10^{-1} \times \frac{\sigma_{yy}}{q_0},\ \bar{\sigma}_{zz} = \frac{\sigma_{zz}}{q_0},\ \bar{\sigma}_{yz} = \frac{\sigma_{yz}}{q_0}$$
$$\text{Aspectratio} = \frac{L}{h},\ \bar{z} = \frac{z}{h} \tag{43}$$

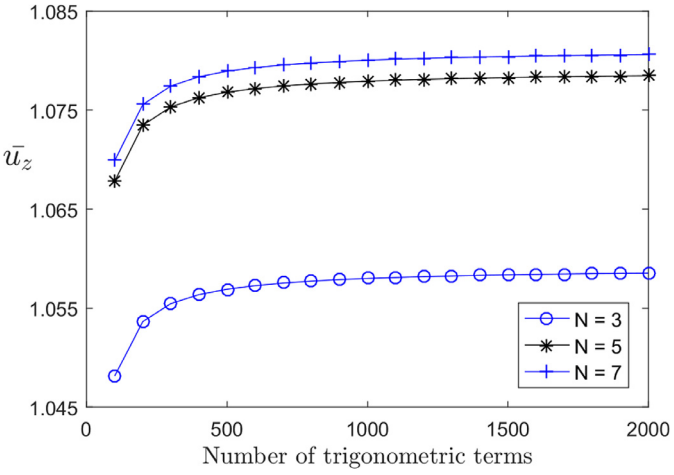

Fig. 3. Convergence of transverse displacement $\bar{u}_z$ at (x=0, y=L/2, z=0) of a C – C (0/90°) laminated square beam with L/h=10 subjected to uniform load for various order expansions.

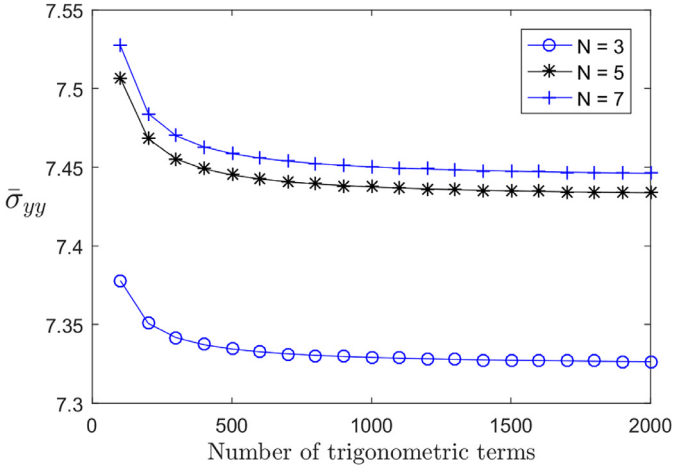

Fig. 4. Convergence of axial stress $\bar{\sigma}_{yy}$ at (x = 0, y = L/2, z = - h/2) of a C – C (0/90°) laminated square beam with L/h = 10 subjected to uniform load for various order expansions.

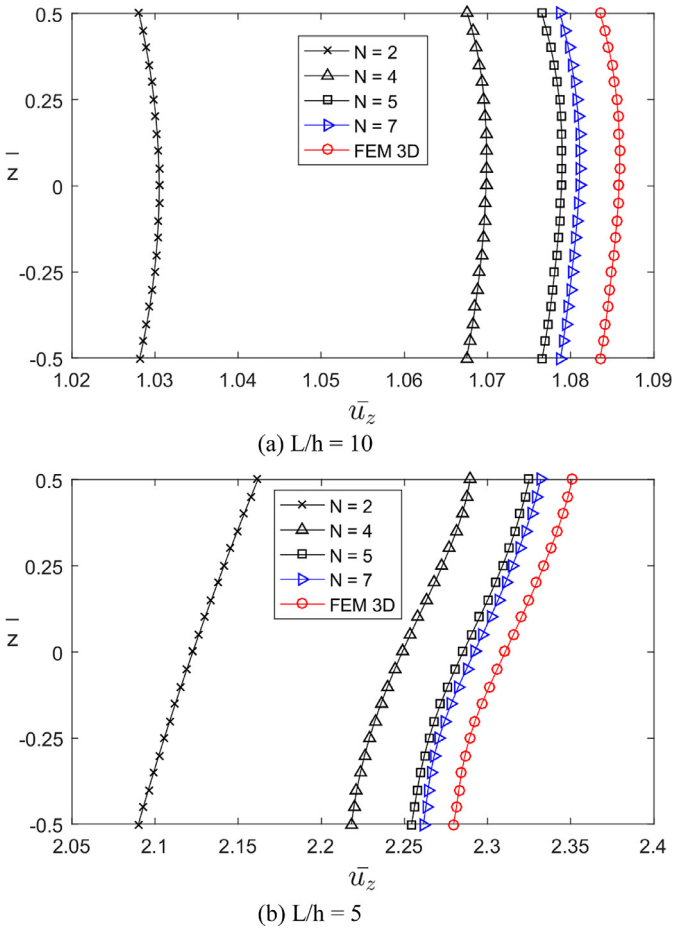

Fig. 5. Distribution of the transverse displacement $\bar{u}_z$ at (x = 0, y = L/2, z) through the thickness of a C – C (0/90°) laminated square beam subjected to uniform load for aspect ratios 10 and 5.

The boundary conditions are denoted by the letters C and S. For example, C – S indicates a beam clamped at y = 0 and simply supported at y = L. Fig. 2 shows the location of the points of evaluation of the displacements and stresses provided in this paper.

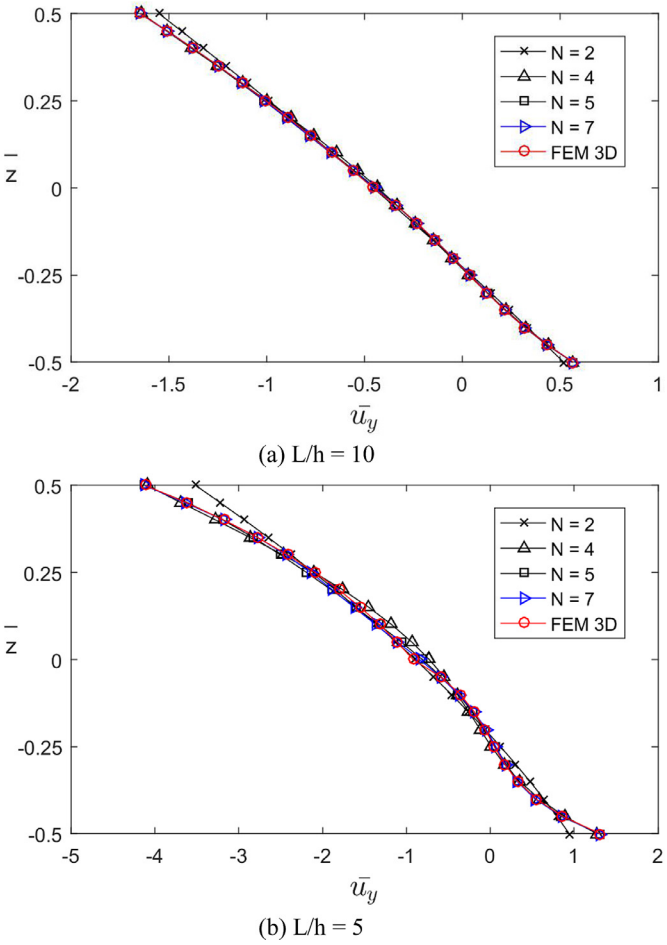

Fig. 6. Distribution of the axial displacement $\bar{u}_y$ at (x = 0, y = L/4, z) through the thickness of a C – C (0/90°) laminated square beam subjected to uniform load for aspect ratios 10 and 5.

Table 2
Convergence of transverse displacement $\bar{u}_z$ at (x = 0, y = L/2, z = 0), axial stress $\bar{\sigma}_{yy}$ at (x = 0, y = L/2, z = - h/2), transverse normal stress $\bar{\sigma}_{zz}$ t (x = 0, y = L/2, z = h/2) and axial displacement $\bar{u}_y$ at (x = 0, y = L/4, z = h/2) for a C – C (0/90°) laminated square beam with L/h = 10 subjected to a uniform load.

Number of terms	$\bar{u}_z$	$\bar{\sigma}_{yy}$	$\bar{\sigma}_{zz}$	$\bar{u}_y$
400	1.0672	7.4178	0.88559	16.339
600	1.0681	7.4138	0.88258	16.352
1000	1.0688	7.4105	0.87987	16.362
1500	1.0692	7.4089	0.87845	16.367
2500	1.0695	7.4076	0.87730	16.372
4000	1.0697	7.4069	0.87664	16.374
6000	1.0698	7.4065	0.87628	16.375
10,000	1.0698	7.4062	0.87599	16.376

3.2. Convergence analysis

Figs. 3 and 4 show the transverse displacement and axial stress of a C – C (0/90°) laminated beam as the number of trigonometric terms in the Fourier series is increased. The beam has an aspect ratio L/h = 10 and is subjected to uniform load in z = h/2. The discontinuities introduced in the displacement functions slow down the convergence of the Fourier series. For this reason, the convergence is much slower compared to an ordinary Navier-type solution. The order expansion N does not seem to greatly influence the speed of convergence, only the final result. Table 2 presents

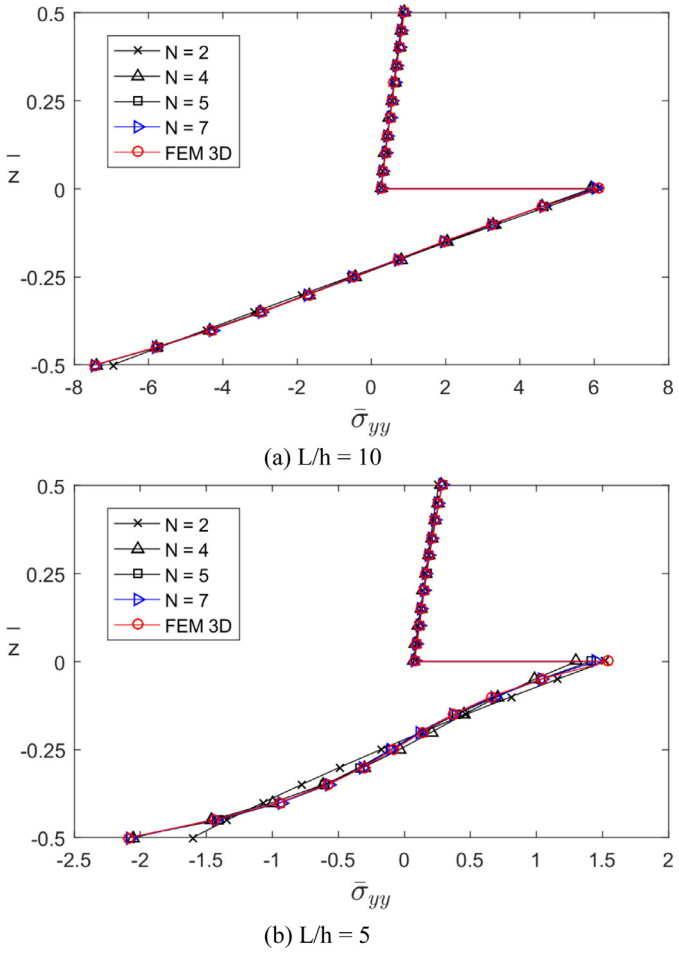

Fig. 7. Distribution of the axial stress $\bar{\sigma}_{yy}$ at (x = 0, y = L/2, z) through the thickness of a C – C (0/90°) laminated square beam subjected to uniform load for aspect ratios 10 and 5.

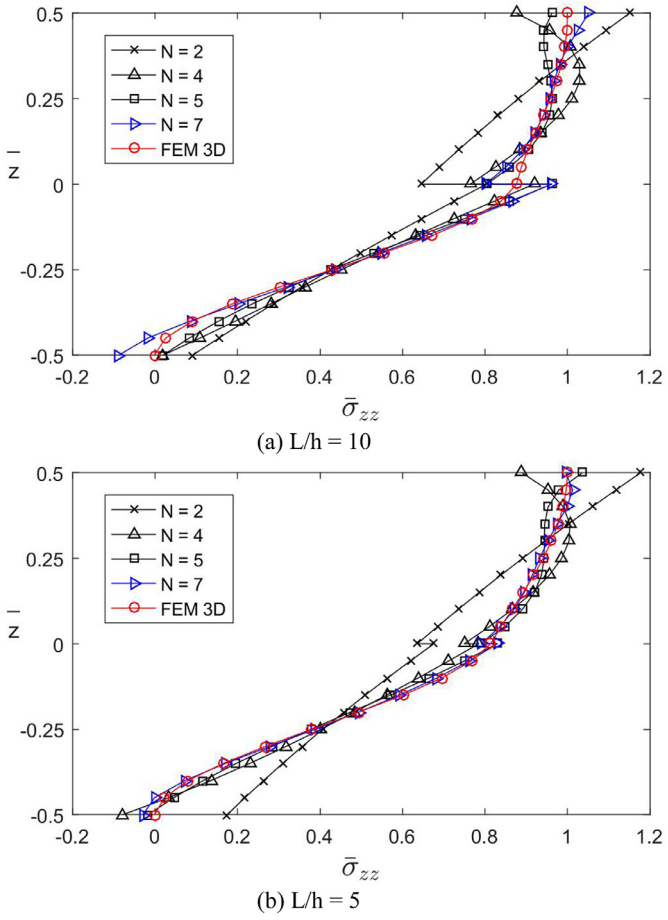

Fig. 8. Distribution of the transverse normal stress $\bar{\sigma}_{zz}$ at (x = 0, y = L/2, z) through the thickness of a C – C (0/90°) laminated square beam subjected to uniform load for aspect ratios 10 and 5.

numerical results for the displacements and stresses as the number of terms in the Fourier series is increased for N = 4. The transverse normal stress $\bar{\sigma}_{zz}$ is seen to converge slowly. At least 4 significant figures can be expected from the numerical results when the number of trigonometric terms is p = 10000, except for the transverse stress $\bar{\sigma}_{zz}$, and this number of terms is further used in the manuscript.

3.3. Clamped – clamped laminated beam

In order to assess the validity of the results, a 3D finite element solution for the static analysis of the laminated beam has been obtained using ANSYS commercial code. The 20-node brick element is used to model the beam. The mesh is such that doubling the elements yields a change lower than 0.05% in $(\bar{\sigma}_y)_{max}$. 350,000 elements were used in order to obtain sufficiently accurate results. Table 3 presents values of displacements and stresses at the specified points of a C – C (0/90°) laminated beam by using the present model, and the corresponding results obtained by the 3D finite element solution. For a beam with L/h = 10, close agreement is obtained for the transverse displacement, axial stress and axial displacement. Slightly higher deviation in transverse normal stress results between 3D finite element solution and the present model are observed. The accuracy of the transverse normal stress is higher for a beam with L/h = 5 than for L/h = 10. On the other hand, the axial stress has higher deviations for thicker beams.

Table 3
Comparison of transverse displacement $\bar{u}_z$ at (x = 0, y = L/2, z = 0), axial stress $\bar{\sigma}_{yy}$ at (x = 0, y = L/2, z = - h/2), transverse normal stress $\bar{\sigma}_{zz}$ at (x = 0, y = L/2, z = h/2) and axial displacement $\bar{u}_y$ at (x = 0, y = L/4, z = h/2) for a C – C (0/90°) laminated square beam subjected to uniform load with aspect ratios 10 and 5.

L/h	Model	$\bar{u}_z$	$\bar{\sigma}_{yy}$	$\bar{\sigma}_{zz}$	$\bar{u}_y$
10	FEM 3D	1.086	7.452	1.000	1.645
	N = 2	1.031	6.966	1.150	1.550
	N = 3	1.059	7.324	1.160	1.598
	N = 4	1.070	7.406	0.876	1.638
	N = 5	1.079	7.431	0.962	1.645
	N = 6	1.079	7.434	1.083	1.646
	N = 7	1.081	7.443	1.052	1.647
5	FEM 3D	2.311	2.090	1.000	4.115
	N = 2	2.123	1.603	1.177	3.515
	N = 3	2.226	1.949	1.085	3.984
	N = 4	2.249	2.052	0.890	4.095
	N = 5	2.285	2.080	1.036	4.125
	N = 6	2.288	2.075	1.039	4.119
	N = 7	2.292	2.081	0.996	4.122

Fig. 5 shows the distribution of transverse displacement across the thickness of a C - C (0/90°) beam with L/h = 5 and 10. The order expansion is given by N and the corresponding 3D finite element solution is also plotted. As expected, more accurate solutions are obtained by using a higher order expansion. Fig. 6 shows the distribution of the axial displacement across the thickness of a C -

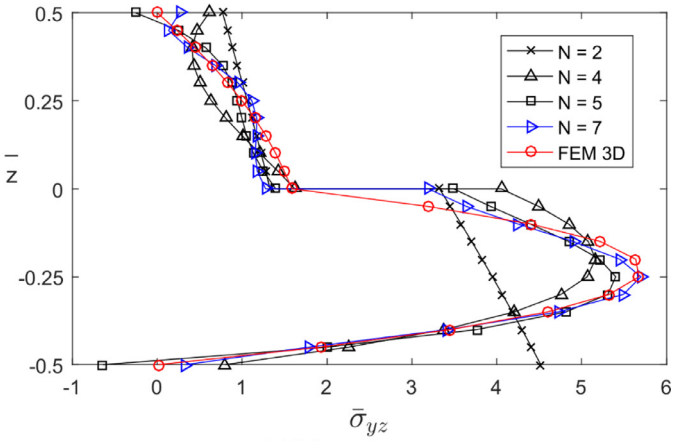

(a) L/h = 10

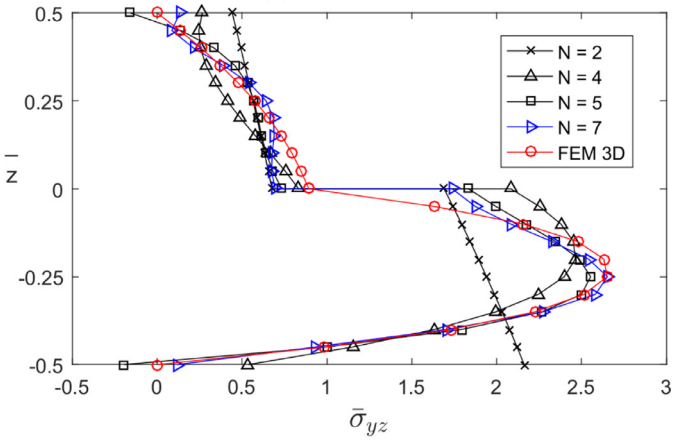

(b) L/h = 5

Fig. 9. Distribution of the transverse shear stress $\bar{\sigma}_{yz}$ at (x = 0, y = L/4, z) through the thickness of a C – C (0/90°) laminated square beam subjected to uniform load for aspect ratios 10 and 5.

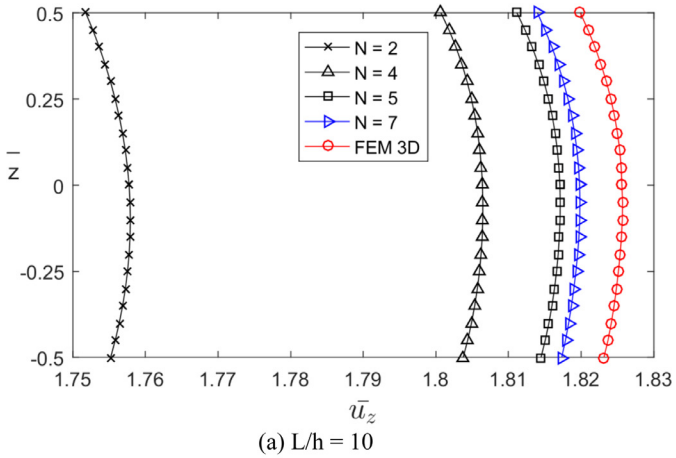

(a) L/h = 10

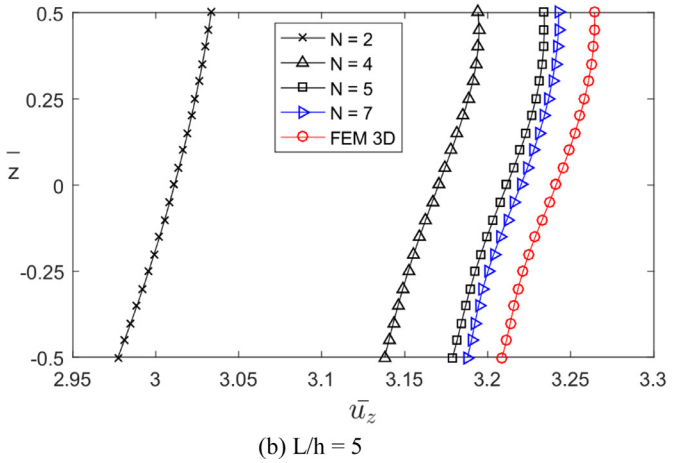

(b) L/h = 5

Fig. 10. Distribution of the transverse displacement $\bar{u}_z$ at (x = 0, y = L/2, z) through the thickness of a C – S (0/90°) laminated square beam subjected to uniform load for aspect ratios 10 and 5.

C (0/90°) beam. In this case, accurate distributions are obtained by using an order expansion N = 5 or higher. Fig. 7 shows the distribution of the axial stress across the thickness of a C – C (0/90°) beam. For a beam with L/h = 10, accurate axial stresses are obtained for N = 4. On the other hand, for a thicker beam with L/h = 5 the error increases, and higher order expansions are required.

Fig. 8 shows the distribution of the transverse normal stress across the thickness of a C - C (0/90°) beam. While the other stresses and displacements are obtained more accurately for beams with higher aspect ratio, i.e. slender beams, accurate results for the transverse normal stress are obtained for beams with lower aspect ratio, i.e. for L/h = 5. Close agreement is obtained by using an order expansion N = 7. Fig. 9 shows the distribution of the transverse shear stress across the thickness of a C – C (0/90°) beam. The maximum shear stress is predicted accurately by using an order expansion N = 7.

3.4. Clamped – simply supported laminated beam

Table 4 presents values of displacement and stresses at certain points of a C – S (0/90°) laminated beam for different aspect ratios, as obtained by the present model and by a 3D finite element solution. Close agreement is obtained for the transverse and axial displacements, as well as for the axial stress. Figs. 10 and 11 show the distribution of the transverse displacement and transverse normal stress across the thickness of a C - S (0/90°). Similar trends as for C – C beams are observed, with the transverse normal stress in close agreement with the 3D finite element solution for a beam with L/h = 5.

Table 4
Comparison of transverse displacement $\bar{u}_z$ at (x = 0, y = L/2, z = 0), axial stress $\bar{\sigma}_{yy}$ at (x = 0, y = L/2, z = - h/2), transverse normal stress $\bar{\sigma}_{zz}$ at (x = 0, y = L/2, z = h/2) and axial displacement $\bar{u}_y$ at (x = 0, y = L/4, z = h/2) for a C – S (0/90°) laminated square beam subjected to uniform load with aspect ratios 10 and 5.

L/h	Model	$\bar{u}_z$	$\bar{\sigma}_{yy}$	$\bar{\sigma}_{zz}$	$\bar{u}_y$
10	FEM 3D	1.826	11.45	1.000	2.756
	N = 2	1.758	10.92	1.124	2.636
	N = 3	1.792	11.30	1.216	2.695
	N = 4	1.806	11.38	0.872	2.750
	N = 5	1.817	11.42	0.905	2.758
	N = 6	1.817	11.42	1.113	2.758
	N = 7	1.820	11.43	1.094	2.760
5	FEM 3D	3.241	3.334	1.000	5.766
	N = 2	3.011	2.814	1.172	5.006
	N = 3	3.136	3.180	1.102	5.586
	N = 4	3.170	3.282	0.887	5.776
	N = 5	3.212	3.316	1.019	5.798
	N = 6	3.214	3.314	1.048	5.789
	N = 7	3.220	3.321	1.008	5.792

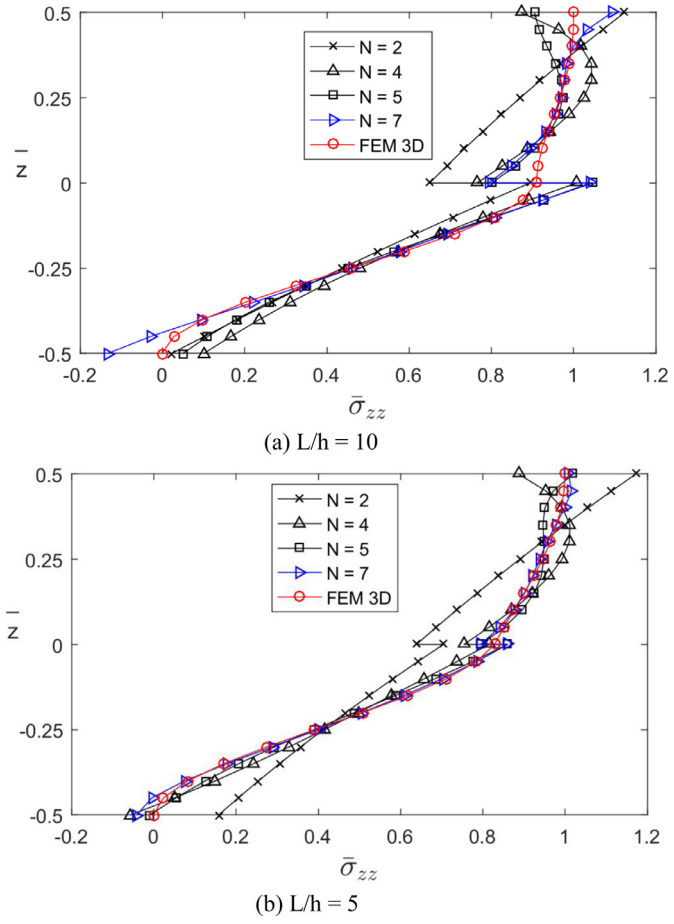

Fig. 11. Distribution of transverse normal stress $\bar{\sigma}_{zz}$ at (x = 0, y = L/2, z) through the thickness of a C – S (0/90°) laminated square beam subjected to uniform load for aspect ratios 10 and 5.

4. Conclusions

An analytical solution for the bending of thick laminated beams with clamped boundary conditions at either of the beam's edges has been presented. Deformation theories of arbitrary order are considered using Carrera Unified Formulation (CUF). The governing equations are obtained by employing the principle of virtual work. In order to account for clamped or mixed boundary conditions at the beam's edges, the boundary discontinuous Fourier approach is used. The results are compared with a 3D finite element solution for validation.

The important conclusions that emerge from this paper can be summarized as follows:

(a) Accurate values of the axial and transverse displacement for clamped laminated beams can be obtained by the present model.
(b) The transverse normal stresses obtained by the present theory are not very accurate for long, slender beams. If required, these stresses can be obtained via the equations of equilibrium.
(c) The boundary discontinuous method can be considered a generalization of the Navier solution, being able to obtain analytical solutions for beams with clamped edges. For simply supported edges, the governing equations of the present method reduce to those of a Navier solution.
(d) In the case of clamped beams, the boundary discontinuous method requires a higher computational effort compared to Navier-type solutions, but it is much lower than the effort required for a 3D finite element solution.

Further studies need to be performed to assess the accuracy of the present model for the analysis of functionally graded and thin-walled beams.

Acknowledgment

This paper is dedicated to Professor Reaz Chaudhuri for his outstanding contribution to computational mechanics.

References

Arya, H., Shimpi, R.P., Naik, N.K., 2002. A zigzag model for laminated composite beams. Compos. Struct. 56, 21–24.
Aydogdu, M., 2009. A new shear deformation theory for laminated composite plates. Compos. Struct. 89, 94–101.
Carrera, E., 2003. Theories and finite elements for multilayered plates and shells. A unified compact formulation with numerical assessment and benchmarking. Arch. Comput. Methods Eng. 10, 215–296.
Carrera, E., 2005. Transverse normal strain effects on thermal stress analysis of homogeneous and layered plates. AIAA J. 43.
Carrera, E., Boscolo, M., Robaldo, A., 2007. Hierarchic multilayered plate elements for coupled multifield problems of piezoelectric adaptive structures. Formulation and numerical assessment. Arch. Comput. Methods Eng. 14, 383–430.
Carrera, E., Brischetto, S., Nali, P., 2008. Variational statements and computational models for multifield problems and multilayered structures. Mech. Adv. Mater. Struct. 15, 192–198.
Carrera, E., Cinefra, M., Petrolo, M., Zappino, E., 2014. Finite Element Analysis of Structures through Unified Formulation. Wiley, Chichester, United Kingdom.
Carrera, E., Filippi, M., Zappino, E., 2013. Laminated beam analysis by polynomial, trigonometric, exponential and zig-zag theories. Eur. J. Mech. A/Solids 41, 58–69.
Carrera, E., Giunta, G., 2010. Refined beam theories based on a unified formulation. Int. J. Appl. Mech. 2, 117–143.
Carrera, E., Giunta, G., Nali, P., Petrolo, M., 2010. Refined beam elements with arbitrary cross-section geometries. Comput. Struct. 88, 283–293.
Carrera, E., Giunta, G., Petrolo, M., 2011. Beam Structures: Classical and Advanced Theories. Wiley, Chichester, United Kingdom.
Carrera, E., Petrolo, M., 2012. Refined beam elements with only displacement variables and plate/shell capabilities. Meccanica 47, 537–556.
Catapano, A., Giunta, G., Belouettar, S., Carrera, E., 2011. Static analysis of laminated beams via a unified formulation. Compos. Struct. 94, 75–83.
Chaudhuri, R.A., 1989. On boundary-discontinuous double Fourier series solution to a system of completely coupled P.D.E.'s. Int. J. Eng. Sci. 27, 1005–1022.
Chaudhuri, R.A., 1994. Effect of boundary constraint on the frequency response of moderately thick flat laminated panels. Compos. Eng. 4, 417–428.
Chaudhuri, R.A., 2002. On the roles of complementary and admissible boundary constraints in Fourier solutions to the boundary value problems of completely coupled rTH order PDEs. J. Sound Vib. 251, 261–313.
Chaudhuri, R.A., Abu-Arja, K.R., 1991. Static analysis of moderately-thick finite antisymmetric angle-ply cylindrical panels and shells. Int. J. Solids Struct. 28, 1–15.
Chaudhuri, R.A., Balaraman, K., Kunukkasseril, V.X., 2005. A combined theoretical and experimental investigation on free vibration of thin symmetrically laminated anisotropic plates. Compos. Struct. 67, 85–97.
Chaudhuri, R.A., Kabir, H.R.H., 1989. On analytical solutions to boundary-value problems of doubly-curved moderately-thick orthotropic shells. Int. J. Eng. Sci. 27, 1325–1336.
Chaudhuri, R.A., Kabir, H.R.H., 1992. A boundary-continuous-displacement based Fourier analysis of laminated doubly-curved panels using classical shallow shell theories. Int.l J. Eng. Sci. 30, 1647–1664.
Chaudhuri, R.A., Kabir, H.R.H., 1993a. Vibration of clamped moderately thick general cross-ply plates using a generalized Navier approach. Compos. Struct. 24, 311–321.
Chaudhuri, R.A., Kabir, H.R.H., 1993b. A boundary discontinuous Fourier solution for clamped transversely isotropic Mindlin plates. Int. J. Solids Struct. 30, 287–297.
Chaudhuri, R.A., Kabir, H.R.H., 1993c. Boundary-discontinuous Fourier analysis of doubly-curved panels using classical shallow shell theories. Int. J. Eng. Sci. 31, 1551–1564.
Chaudhuri, R.A., Kabir, H.R.H., 1993d. Sensitivity of the response of moderately thick cross-ply doubly-curved panels to lamination and boundary constraint-II. Appl. - Int. J. Solids Struct. 30, 273–286.
Chaudhuri, R.A., Kabir, H.R.H., 1993e. Sensitivity of the response of moderately thick cross-ply doubly-curved panels to lamination and boundary constraint-I. Theory - Int. J. Solids Struct. 30, 263–272.
Chaudhuri, R.A., Kabir, H.R.H., 1994. Static and dynamic Fourier analysis of finite cross-ply doubly curved panels using classical shallow shell theories. Compos. Struct. 28, 73–91.
Chaudhuri, R.A., Kabir, H.R.H., 2005. Effect of boundary constraint on the frequency response of moderately thick doubly curved cross-ply panels using mixed Fourier solution functions. J. Sound Vibr. 283, 263–293.
Filippi, M., Pagani, A., Petrolo, M., Colonna, G., Carrera, E., 2015. Static and free vibration analysis of laminated beams by refined theory based on Chebyshev polynomials. Compos. Struct. 132, 1248–1259.

Giunta, G., Biscani, F., Belouettar, S., Ferreira, A.J.M., Carrera, E., 2013a. Free vibration analysis of composite beams via refined theories. Compos. 44, 540–552.
Giunta, G., de Pietro, G., Nasser, H., Belouettar, S., Carrera, E., Petrolo, M., 2016. A thermal stress finite element analysis of beam structures by hierarchical modelling. Compos. Part B 95, 179–195.
Giunta, G., Koutsawa, Y., Belouettar, S., Hu. Static, H., 2013b. Free vibration and stability analysis of three-dimensional nano-beams by atomistic refined models accounting for surface free energy effect. Int. J. Solids Struct. 50, 1460–1472.
Giunta, G., Metla, N., Koutsawa, Y., Belouettar, S., 2013c. Free vibration and stability analysis of three-dimensional sandwich beams via hierarchical models. Compos. Part B 47, 326–338.
Hutchinson, J.R., 1981. Transverse vibrations of beams, exact versus approximate solutions. J. Appl. Mech. 48, 923–928.
Hutchinson, J.R., Zillmer, S.D., 1986. On the transverse vibration of beams with rectangular cross-section. J. Appl. Mech. 53, 39–44.
Ibrahim, S.M., Carrera, E., Petrolo, M., Zappino, E., 2012. Buckling of composite thin walled beams by refined theory. Compos. Struct. 94, 563–570.
Kabir, H.R.H., 1994. Free vibration of clamped, moderately thick, arbitrarily laminated plates using a generalized Navier's approach. J. Sound Vibr. 171, 397–410.
Kabir, H.R.H., Al-Khaleefi, A.M., Chaudhuri, R.A., 2003. Frequency response of a moderately thick antisymmetric cross-ply cylindrical panel using mixed type of Fourier solution functions. J. Sound Vibr. 259, 809–828.
Kabir, H.R.H., Chaudhuri, R.A., 1991a. A generalized Navier's approach for solution of clamped moderately-thick cross-ply plates. Comput. Struct. 17, 351–366.
Kabir, H.R.H., Chaudhuri, R.A., 1991b. Free vibration of shear-flexible anti-symmetric angle-ply doubly curved panels. Int. J. Solids Struct. 28, 17–32.
Kabir, H.R.H., Chaudhuri, R.A., 1993. A direct Fourier approach for the analysis of thin finite-dimensional cylindrical panels. Comput. Struct. 46, 279–287.
Kabir, H.R.H., Chaudhuri, R.A., 1994. On Gibbs-phenomenon-free Fourier solution for finite shear-flexible laminated clamped curved panels. Int.l J. Eng. Sci. 32, 501–520.
Khdeir, A.A., Reddy, J.N., 1997. An exact solution for the bending of thin and thick cross-ply laminated beams. Compos. Struct. 37, 195–203.
Oktem, A.S., Chaudhuri, R.A., 2007a. Fourier analysis of thick cross-ply Levy type clamped doubly-curved panels. Compos. Struct. 80, 489–503.
Oktem, A.S., Chaudhuri, R.A., 2007b. Boundary discontinuous Fourier analysis of thick cross-ply clamped plates. Compos. Struct. 82, 539–548.
Oktem, A.S., Chaudhuri, R.A., 2007c. Fourier solution to a thick cross-ply Levy type clamped plate problem. Compos. Struct. 79, 481–492.
Oktem, A.S., Chaudhuri, R.A., 2008. Effect of inplane boundary constraints on the response of thick general (unsymmetric) cross-ply plates. Compos. Struct. 83, 1–12.
Oktem, A.S., Chaudhuri, R.A., 2009. Sensitivity of the response of thick cross-ply doubly curved panels to edge clamping. Compos. Struct. 87, 293–306.
Polit, O., Gallimard, L, Vidal, P., D'Ottavio, M., Giunta, G., Belouettar, S., 2015. An analysis of composite beams by means of hierarchical finite elements and a variables separation method. Comput. Struct. 158, 15–29.
Reddy, J.N., 2004. Mechanics of Laminated Composite Plates: Theory and Analysis, 2nd ed CRC Press, Boca Raton FL.
Rychter, Z., 1987. On the shear coefficient in beam bending. Mech. Res. Commun. 14, 379–385.
Sayyad, A.S., Ghugal, Y.M., 2011. Effect of transverse shear and transverse normal strain on bending analysis of cross-ply laminated beams. Int. J. Appl. Math. Mech. 7, 85–118.
Shimpi, R.P., Ghugal, Y.M., 2001. A new layerwise trigonometric shear deformation theory for two-layered cross-ply beams. Compos. Sci. Technol. 61, 1271–1283.